Yen and Voltz *EURASIP Journal on Wireless Communications and Networking* 2011, **2011**:189
http://jwcn.eurasipjournals.com/content/2011/1/189

EURASIP Journal on Wireless Communications and Networking
a SpringerOpen Journal

RESEARCH Open Access

Indoor positioning based on statistical multipath channel modeling

Chia-Pang Yen[1*] and Peter J Voltz[2]

Abstract

In order to estimate the location of an indoor mobile station (MS), estimated time-of-arrival (TOA) can be obtained at each of several access points (APs). These TOA estimates can then be used to solve for the location of the MS. Alternatively, it is possible to estimate the location of the MS directly by incorporating the received signals at all APs in a direct estimator of position. This article presents a deeper analysis of a previously proposed maximum likelihood (ML)-TOA estimator, including a uniqueness property and the behavior in nonline-of-sight (NLOS) situations. Then, a ML direct location estimation technique utilizing all received signals at the various APs is proposed based on the ML-TOA estimator. The Cramer-Rao lower bound (CRLB) is used as a performance reference for the ML direct location estimator.

Keywords: indoor positioning, maximum likelihood (ML), time-of-arrival (TOA), direct location estimation

1 Introduction

With the emergence of location-based applications and the need for next-generation location-aware wireless networks, location finding is becoming an important problem. Indoor localization has recently started to attract more attention due to increasing demands from security, commercial and medical services. For example, next generation corporate wireless local area networks (WLAN) will utilize location-based techniques to improve security and privacy [1]. The requirement for high accuracy positioning in complex multipath channels and nonline-of-sight (NLOS) situations has made the task of indoor localization very challenging as compared to outdoor environments.

Conventionally, the positioning problem is solved via an indirect (two-step) parameter estimation scheme. First, the time-of-arrival (TOA) estimation at each access point (AP) is performed. The TOA estimator estimates the first arriving path delay, which corresponds to the line-of-sight (LOS) distance between the transmitter and the receiver assuming the LOS path exists. Then, these TOA estimates from each AP are transmitted to a central terminal at which the location estimation is carried out by various algorithms, such as trilateration or least squares fitting, etc. [2,3]. Recently, the direct location estimation method has been proposed as another aspect to the positioning problem [4]. Unlike the indirect methods which split the location estimation efforts between the APs and the central terminal, the direct positioning methods rely only on the central terminal to perform the location estimation task. The APs just relay the received signals to the central terminal for it to estimate the location of the mobile station (MS). It has been shown that the direct method can outperform the indirect method [4].

For the indirect positioning methods, the first step is to obtain an accurate TOA estimation. To separate closely spaced channel paths, super-resolution techniques [5], such as multiple signal classification (MUSIC), etc. [6-8], are reported to be able to significantly improve the TOA estimations as compared to the conventional autocorrelation approach [9].

Maximum likelihood (ML) is a natural approach for TOA estimation but in order to resolve the multiparameter issue that seems natural to the multipath environments, a novel ML-TOA estimator that only requires a one-dimensional search is proposed in [10]. The ML-TOA technique estimates only the first arriving path delay based on the observation that this parameter is the only quantity needed for positioning. It was found that in

* Correspondence: chiapang.yen@itri.org.tw
[1]ITRI (Industrial Technology Research Institute), 195, Sec. 4, Chung Hsing Rd., Chutung, Hsinchu 310, Taiwan
Full list of author information is available at the end of the article

dense multipath environments, the ML-TOA estimation outperforms the super-resolution methods discussed in [11,12]. The effect of considering only the first arriving path delay in positioning was studied in [13]. Based on the analyses of the Cramer-Rao lower bound (CRLB), the authors showed that if the paths are correlated then including other paths could improve the TOA estimation accuracy, however, they also pointed out that doing so "would not help enhance the accuracy significantly but merely increase the computational complexity."

In this article, several important properties pertaining to the ML-TOA estimator that were previously left unanswered are established. First is the uniqueness of the ML-TOA estimator. For TOA estimation in multipath environments, not only the additive noise but also the multipath channels are random. Therefore, it is not obvious that the estimates converge to the exact parameter when signal-to-noise ratio (SNR) increases. Here, we demonstrate that the ML-TOA estimation provides the unique, correct TOA in the absence of noise provided the channel statistics are known. The effects of the NLOS situations are also discussed. The NLOS situation is another major challenge for indoor positioning for it can cause large TOA estimation bias that in turn result in large location estimation errors [14]. There are optimization methods which can be used to mitigate the error due to NLOS. In [15,16], the optimization is carried out with respect to the unknown mobile location or the NLOS bias. In [13,17,18], statistical estimation methods are proposed in the case that the statistical knowledge such as the propagation scattering models or the NLOS delays statistics are known. In this article, the proposed ML-TOA is shown to be able to incorporate the statistics of NLOS channels automatically and thus reduce the estimation bias due to NLOS path delays.

The direct positioning method has just started to emerge as an interesting research topic and has been shown to provide improvement in the location estimation accuracy. Thus, in this article, in addition to the indirect (two-step) method, we also propose a direct ML positioning algorithm based on the ML-TOA estimator. In [19], the authors proposed a direct positioning method for orthogonal-frequency-division-multiplexing (OFDM) signals. There, the APs are assumed to be equipped with antenna arrays, the source is located in the far field and the channel power delay profile has a significant path while the rest paths are ignored. Here, we assume that each AP has a single antenna and the channel has multipath. It is shown that our proposed ML direct location estimator also posesses the uniqueness property thus its estimates are reliable. Furthermore, the CRLB of the direct location estimator is used as a performance reference. The simulation results show that the proposed direct positioning method has better performance than the indirect method and is close to the CRLB for some channels. While we focus on an OFDM signal structure, which is mathematically convenient and has not been studied extensively in the indoor localization problem, the approach can be generalized to any signal type.

The remainder of the article is organized as follows. Section 2 presents the mathematical formulation of the TOA estimation problem and the ML-TOA estimator. Section 3 presents analyses of the proposed ML-TOA estimator including the uniqueness property, the behavior of the cost function and the effects of the NLOS situations. In Section 4, a ML direct positioning algorithm is proposed based on the ML-TOA estimation algorithm. The uniqueness property associated with the ML direct location estimator is also shown. In Section 5, the performance of ML-TOA estimator and the proposed direct algorithm are demonstrated through computer simulations. Finally, conclusions are presented in Section 6.

2 ML-TOA estimation

One OFDM symbol duration is $T + T_G$, where T_G is the guard interval, and T is the receiver integration time over which the sub-carriers are orthogonal. A single symbol of the transmitted OFDM signal is assumed to have N sub-carriers with transmitted sequence vector $\mathbf{d} = [d_0\ d_1 \cdots d_{N\text{-}1}]^T$. Assume that the signal is received after passing through a multipath channel with impulse response $h(t) = \sum_{i=0}^{L-1} a_i \delta(t - \tau_i)$ in which $0 \le \tau_0 \le \tau_1 \le \cdots \le \tau_{L\text{-}1} \le T_G$ and a_i is the complex channel gain of the ith path. After the standard receiver sampling, guard interval removal and fast-Fourier-transformation (FFT) processing, the kth element of the FFT output vector is (see [10] for details)

$$\gamma_k = d_k \left(\sum_{i=0}^{L-1} a_i e^{-j\frac{2\pi}{T} k\tau_i} \right) + n_k, \tag{1}$$

where n_k is complex Gaussian noise with variance $\sigma^2 = N_0$.

Conventional ML estimation is formulated in such a way that the unknown parameter is a multivariate vector, i.e., $\theta = [a_0 \ldots a_{L\text{-}1}\ \tau_0 \ldots \tau_{L\text{-}1}]^T$. When the number of paths L is large, the computational complexity becomes prohibitive. However, only the first path delay, τ_0, is required for location estimation purpose. Therefore, we focus the ML estimation on the TOA only, assuming a statistical model of the channel.

In this section, we assume a direct LOS path exists. The case of NLOS will be discussed in Section 3. Denote τ_0 as the TOA, the path delay that corresponds to the first arriving path. Then, referenced to τ_0, the

other path delays can be written as $\tau_i = \tau_0 + (\tau_i - \tau_0) = \tau_0 + \bar{\tau}_i$. Equation (1) then becomes

$$y_k = H_k d_k e^{-j\frac{2\pi}{T}k\tau_0} + n_k, \tag{2}$$

where H_k is given by $H_k = \sum_{i=0}^{L-1} a_i e^{-j\frac{2\pi}{T}k\bar{\tau}_i}$ and is the zero delay frequency response at the kth subcarrier.

Define the subcarrier frequency response vector as $\mathbf{h} = [H_0\ H_1\ \ldots\ H_{N-1}]^T$. We assume at first that $\mathbf{h}$ is a zero mean, circular complex Gaussian vector with known covariance matrix $\mathbf{K_h} = \mathbb{E}\left\{\mathbf{h}\mathbf{h}^H\right\}$, where the H denotes Hermitian transpose [20]. This Gaussian assumption is for mathematical development and the proposed TOA estimator, as was demonstrated in [10] for Ray-Trace data, performs well in practical situations. Equation (2) can then be used to express the complete FFT output vector as

$$\mathbf{y} = \mathbf{G}(\tau_0)\mathbf{D}\mathbf{h} + \mathbf{n}, \tag{3}$$

where

$\mathbf{G}(\tau_0) = \text{diag}\left\{1, e^{-j\frac{2\pi}{T}\tau_0}, e^{-j\frac{2\pi}{T}2\tau_0}, \ldots, e^{-j\frac{2\pi}{T}(N-1)\tau_0}\right\}$ and $\mathbf{D}$ = diag $\{d_0, d_1, d_2, \ldots, d_{N-1}\}$ consists of the transmitted symbols. We shall assume that time delay estimation is performed on an OFDM training symbol so that $\mathbf{D}$ is known. As shown in [10], the ML solution for TOA τ_0 is

$$\hat{\tau}_0 = \arg\max_{\tau} Q(\tau) = \arg\max_{\tau} \mathbf{y}^H \mathbf{G}(\tau)\mathbf{F}\mathbf{G}(\tau)^H\mathbf{y}, \tag{4}$$

where the cost function of the estimator is defined as

$$Q(\tau) \triangleq \mathbf{y}^H \mathbf{G}(\tau)\mathbf{F}\mathbf{G}(\tau)^H\mathbf{y}, \tag{5}$$

where $\mathbf{F} = \mathbf{D}\mathbf{R}\,(\sigma^2\mathbf{I} + \mathbf{R}^H\mathbf{D}^H\mathbf{D}\mathbf{R})^{-1}\mathbf{R}^H\mathbf{D}^H$ and $\mathbf{R}$ is a rank $L(< N)$ factor of $\mathbf{K_h}$ as $\mathbf{K_h} = \mathbf{R}\mathbf{R}^H$.

3 Performance characteristics of the ML-TOA estimator

When estimating TOA in a dense multipath environment, the accuracy is impacted not only by the noise, but also by the presence of the many echoes of the signal due to the multipath. In this section, we first demonstrate that when noise is absent and we are in the presence of multipath only, then the proposed estimator yields the correct TOA uniquely, provided the covariance matrix $\mathbf{K_h}$ is exactly known. For the rest of the article, we assume that $\mathbf{D} = \mathbf{I}$ without loss of generality.

3.1 Uniqueness of the ML-TOA estimation

Assume for the present that noise is absent, i.e., $\sigma^2 = 0$. Since $\mathbf{K_h}$ can be factored using the Singular Value Decomposition $\mathbf{K_h} = (\mathbf{U}\mathbf{\Lambda}^{1/2}\mathbf{U}^H)(\mathbf{U}\mathbf{\Lambda}^{1/2}\mathbf{U}^H) = \mathbf{R}\mathbf{R}^H$, the channel can be expressed as

$$\mathbf{h} = \mathbf{R}\mathbf{z}, \tag{6}$$

where $\mathbf{z} \in C^L$ is a zero mean Gaussian random vector with covariance matrix $\mathbb{E}\{\mathbf{z}\mathbf{z}^H\} = \mathbf{I}$ and L is the rank of $\mathbf{K_h}$. In this case, the received FFT output vector will be $\mathbf{y} = \mathbf{G}(\tau_0)\mathbf{h} = \mathbf{G}(\tau_0)\mathbf{R}\mathbf{z}$.

Using this expression and the fact that when noise is absent the $\mathbf{F}$ matrix reduces to $\mathbf{F} = \mathbf{R}\,(\mathbf{R}^H\mathbf{R})^{-1}\,\mathbf{R}^H$ and the fact that $\mathbf{G}^H(\tau)\mathbf{G}(\tau_0) = \mathbf{G}^H(\tau - \tau_0)$, the cost function $Q(\tau)$ in (5) becomes $Q(\tau) = \mathbf{z}^H\,\mathbf{R}^H\mathbf{G}^H(\tau_0)\mathbf{G}(\tau)\mathbf{R}\,(\mathbf{R}^H\,\mathbf{R})^{-1}\,\mathbf{R}^H\mathbf{G}^H(\tau)\mathbf{G}(\tau_0)\mathbf{R}\mathbf{z} = ||\mathbf{P_R}\mathbf{G}^H(\tau - \tau_0)\mathbf{R}\mathbf{z}||^2$ where $\mathbf{P_R} = \mathbf{R}\,(\mathbf{R}^H\,\mathbf{R})^{-1}\,\mathbf{R}^H$ is the orthogonal projector onto the range space of $\mathbf{R}$, i.e., Range ($\mathbf{R}$), and this follows from the fact that $\mathbf{P_R^2} = \mathbf{P_R}$. Since $\mathbf{P_R}$ is an orthogonal projector, it can be seen that given a realization of $\mathbf{z}$, $Q(\tau)$ is maximized if and only if $\mathbf{G}^H\,(\tau - \tau_0)\,\mathbf{R}\mathbf{z} \in$ Range ($\mathbf{R}$). Obviously, this is the case when $\tau = \tau_0$ and the $\mathbf{G}$ matrix reduces to an identity matrix. We would like to investigate whether there are other possible maximizing values of τ.

To simplify the notation, let $\theta = \frac{2\pi}{T}(\tau - \tau_0)$ and define $\mathbf{G}(\theta) \triangleq \mathbf{G}^H(\tau - \tau_0)$. We are looking for conditions on θ such that $\mathbf{G}(\theta)\mathbf{R}\mathbf{z} \in$ Range($\mathbf{R}$), $\theta = 0$ being an obvious solution. We note first that we can convert this problem into the deterministic one of finding conditions on θ such that Range ($\mathbf{G}\,(\theta)\,\mathbf{R}$) $\subseteq$ Range($\mathbf{R}$). Certainly this latter condition is sufficient to guarantee that $\mathbf{G}(\theta)\,\mathbf{R}\mathbf{z} \in$ Range($\mathbf{R}$). It is also true that if Range ($\mathbf{G}(\theta)\mathbf{R}$) $\nsubseteq$ Range($\mathbf{R}$), then $\mathbf{G}(\theta)\mathbf{R}\mathbf{z} \notin$ Range($\mathbf{R}$) with probability one. To see this, note that Range ($\mathbf{G}(\theta)\mathbf{R}$) $\nsubseteq$ Range($\mathbf{R}$) is equivalent to [Range ($\mathbf{R}$)]$^\perp$ $\nsubseteq$ [Range ($\mathbf{G}(\theta)\mathbf{R}$)]$^\perp$ where $\perp$ denotes the orthogonal complement. Let $\mathbf{v}$ denote any non-zero vector such that $\mathbf{v} \in$ [Range ($\mathbf{R}$)]$^\perp$ but $\mathbf{v} \notin$ [Range ($\mathbf{G}(\theta)\mathbf{R}$)]$^\perp$. Then, $\mathbf{v}^H\mathbf{G}(\theta)\mathbf{R} \neq \mathbf{0}$ and the random variable $\mathbf{v}^H\mathbf{G}(\theta)\mathbf{R}\mathbf{z}$ is Gaussian with non-zero variance and will be non-zero with probability one. Therefore, with probability one, $\mathbf{v}^H\,\mathbf{G}(\theta)\mathbf{R}\mathbf{z} \neq 0$ and $\mathbf{G}(\theta)\mathbf{R}\mathbf{z} \notin$ Range($\mathbf{R}$) because it is not orthogonal to $\mathbf{v}$.

Now, the deterministic condition Range ($\mathbf{G}(\theta)\mathbf{R}$) $\subseteq$ Range ($\mathbf{R}$) is equivalent to the existence of some matrix $\mathbf{A}$ such that $\mathbf{G}(\theta)\mathbf{R} = \mathbf{R}\mathbf{A}$. Multiplying on the left by $\mathbf{G}$ yields $\mathbf{G}^2\mathbf{R} = \mathbf{G}\mathbf{R}\mathbf{A} = \mathbf{R}\mathbf{A}^2$, and continuing this operation yields $\mathbf{G}^n\mathbf{R} = \mathbf{R}\mathbf{A}^n$, for all positive integers n. It follows easily that for any polynomial $f(\lambda) = \sum_n c_n\lambda^n$,

$$f(\mathbf{G})\mathbf{R} = \mathbf{R}f(\mathbf{A}), \tag{7}$$

where $f(\mathbf{A}) = \sum_n c_n\mathbf{A}^n$ is a matrix polynomial. From the structure of $\mathbf{G}$, we see that

$$f(\mathbf{G}) = \text{diag}\{f(1), f(e^{j\theta}), f(e^{j2\theta}), \ldots, f(e^{j(N-1)\theta})\}. \tag{8}$$

Equation (7) says that any matrix of the form (8) can multiply **R** on the left, and the resulting matrix $f(\mathbf{G})\mathbf{R}$ satisfies Range $(f(\mathbf{G})\mathbf{R}) \subseteq$ Range $(\mathbf{R})$.

Let us now assume that Range(**R**) includes the flat channel vector $\mathbf{h}_f = \mathbf{1}$ where **1** is a vector with all unit elements. This essentially assumes that a flat fading channel is one of the possible realizations so that there is a vector **z** such that $\mathbf{1} = \mathbf{R}\mathbf{z}$. Multiplying (7) by **z** yields $f(\mathbf{G})\mathbf{1} = \mathbf{R}f(\mathbf{A})\mathbf{z}$ which means that, from (6),

$$f(\mathbf{G})\mathbf{1} = \left[f(1)\ f(e^{j\theta})\ f(e^{j2\theta})\ \cdots\ f(e^{j(N-1)\theta})\right]^T \quad (9)$$

is a realizable channel vector for any polynomial $f(\lambda)$.

Now, let L be the rank of **R** and assume that $L < N$. Then, the N values $\{1, e^{j\theta}, e^{j2\theta},..., e^{j(N-1)\theta}\}$ cannot all be distinct for, if they were, the channel vector (9) could be chosen arbitrarily by suitable choice of interpolating polynomial $f(\lambda)$, contrary to the fact that the realizable channels are restricted to the L dimensional space Range (**R**). This is due to the well-known fact that a polynomial can always be found, which takes arbitrary values on any given set of arguments. In fact, we can see that at most L of the values $\{1, e^{j\theta}, e^{j2\theta},..., e^{j(N-1)\theta}\}$ can be distinct for a similar reason. Now suppose there are actually q distinct values. It follows that the first q values must be distinct because, for example, if $e^{jr\theta} = e^{jp\theta}$ where $r < p \le q$ then $e^{j(p-r)\theta} = 1$ and there will be only $p - r - 1 < q$ distinct values.

We have now shown that there must be an integer $q \le L$ such that $e^{jq\theta} = 1$. Then, the sequence $\{1, e^{j\theta}, e^{j2\theta},..., e^{j(N-1)\theta}\}$ cycles as follows $\{1, e^{j\theta}, e^{j2\theta},..., e^{j(q-1)\theta}, 1, e^{j\theta}, e^{j2\theta},...\}$. Suppose for example that $q = 2$. Then, the sequence is $\{1, e^{j\theta}, 1, e^{j\theta},...,1, e^{j\theta},...\}$. Choose an interpolating polynomial such that $f(1) = 1$ and $f(e^{j\theta}) = -1$. Then, from (9) the vector of alternating plus and minus ones, i.e., $f(\mathbf{G})\mathbf{1} = [1\ -1\ 1\ -1\ 1...]^T$ would be a realizable channel vector. But this highly oscillatory channel frequency response would imply a very large channel delay spread. Therefore, if the delay spread of the channel is not too large, the value $q = 2$ would not be realistic. Similar examples of unrealistic channel frequency response can be constructed for any q greater than 1. Therefore, we are left with $q = 1$ in which case the only solution is $e^{jq\theta} = 1$ so that $\theta = 0$ and the solution is unique. The simulation results in Section 5.1 also demonstrate this uniqueness property of the ML-TOA estimator.

3.2 ML-TOA estimation in NLOS situations

In this section, the effect of NLOS on the ML-TOA estimator is discussed and we show that the NLOS case is very naturally incorporated into the proposed ML-TOA estimator. Recall (1), (2) and (3) which illustrate how the TOA τ_0 is factored out and incorporated into the **G** matrix. These equations were developed with the understanding that τ_0 was the path delay of the direct LOS path. From now on, however, we simply define TOA τ_0 as the time it would take for an electromagnetic wave to travel the straight line that links the MS and AP, whether or not such a direct LOS path actually exists. In the case when a LOS path does not exist, (1) would be modified to read

$$\gamma_k = d_k \left(\sum_{i=1}^{L-1} a_i e^{-j\frac{2\pi}{T}k\tau_i} \right) + n_k, \quad (10)$$

where the $i = 0$ term has been removed since the LOS path is absent. Nevertheless, with τ_0 defined as above, we may still express the actual path delays in terms of τ_0 as $\tau_i = \tau_0 + (\tau_i - \tau_0) = \tau_0 + \bar{\tau}_i$, and we obtain a modified (2) as

$$\gamma_k = H_k d_k e^{-j\frac{2\pi}{T}k\tau_0} + n_k, \quad (11)$$

where H_k is now given by $H_k = \sum_{i=1}^{L-1} a_i e^{-j\frac{2\pi}{T}k\bar{\tau}_i}$, and is the zero delay frequency response at the kth subcarrier when no LOS path is present. We maintain the earlier definition of the subcarrier frequency response vector as $\mathbf{h} = [H_0\ H_1\ ...\ H_{N-1}]^T$ and (11) can be used to express the complete FFT output vector as

$$\mathbf{y} = \mathbf{G}(\tau_0)\mathbf{D}\mathbf{h} + \mathbf{n}. \quad (12)$$

Note that (12) is exactly the same as (3). The only difference in this NLOS case is the modification of the elements of the **h** vector due to the absence of the direct path. The derivation of the ML estimator now follows exactly as the case in which a direct path is present, and the channel statistics as measured by the procedure outlined below will reflect the actual environment, whether or not there is always a direct path present.

In practice, no matter what the multipath structure, the channel covariance matrix $\mathbf{K_h}$ can be estimated offline by averaging measurements at each AP while the MS transmits at some known locations chosen in a random fashion. The detailed procedure is as follows: *Step 1* : For a given, *known*, AP location, measure the received FFT output vector $\mathbf{y}^{(i)}$ at the AP for the ith MS location. *Step 2* : Since, in this measurement phase, both MS and AP locations are known, TOA of the ith MS transmission (at ith location), i.e., $\tau_0^{(i)}$, can be computed by dividing the distance between them by the speed of light, and the $\mathbf{G}^{(i)}$ matrix can be determined by $\mathbf{G}^{(i)} = \mathrm{diag}\left\{1, e^{-j\frac{2\pi}{T}\tau_0^{(i)}}, e^{-j\frac{2\pi}{T}2\tau_0^{(i)}}, \ldots, e^{-j\frac{2\pi}{T}(N-1)\tau_0^{(i)}}\right\}$.

Then, for this ith transmission, the FFT output vector $\mathbf{y}$ in Equation (12) is measured and an estimated snapshot of $\mathbf{h}^{(i)}$ can be found by $\widehat{\mathbf{h}}^{(i)} = (\mathbf{G}^{(i)})^{-1}\mathbf{y}^{(i)} = \mathbf{h}^{(i)} + (\mathbf{G}^{(i)})^{-1}\mathbf{n}^{(i)}$. *Step 3*: After collecting measurements at P different MS locations, the estimated channel covariance matrix is obtained by $\hat{\mathbf{K}}_{\mathbf{h}} = \frac{1}{P}\sum_{i=1}^{P}\widehat{\mathbf{h}}^{(i)}\left(\widehat{\mathbf{h}}^{(i)}\right)^{H}$.

For future reference we now define the NLOS delay. For the NLOS case in which a LOS path does not exist, τ_1 in (10) will be the first arriving path delay. Then, we define "NLOS delay" = τ_1 - τ_0, where τ_0 is the line of sight distance divided by the speed of light, as described above. The NLOS delay is sometimes called the excess delay and is the time difference between the first arriving actual NLOS path and the direct LOS time delay, τ_0.

At this point, we emphasize that the NLOS case is very naturally incorporated into the proposed ML-TOA estimator. Recall that in the entire development, including the estimation procedure for $\hat{\mathbf{K}}_{\mathbf{h}}$ above, TOA is defined as the time it takes for the electromagnetic waves to travel the straight line that links the MS and AP, whether or not such a LOS path actually exists. Therefore, in *Step 2* above the TOA can still be computed given the location of MS and AP even in the absence of a LOS path, since TOA is known whether or not a direct LOS exists. This is based on the idea that motivates the ML-TOA estimation. That is to separate the desired parameter from the statistics of the multipath channel. For the purpose of positioning, the desired parameter is the "generalized" TOA that we defined in the beginning of this section. In this way, the statistical properties of the measured channels will naturally incorporate the NLOS properties of the channel and no extra step or *a prior* information about the NLOS statistics is required to mitigate the NLOS effects. In Section 5.1, we present simulation results which show the TOA estimation performance for both LOS and NLOS cases. Finally, we point out that, since (12) is identical to (3), the uniqueness proof in Section 3.1 applies to the NLOS case as well.

3.3 Properties of the cost function $Q(\tau)$

The TOA estimation is a nonlinear problem and is known to exhibit ambiguities which could result in large errors [21,22]. In the large error regime, the CRLB cannot be attained. In this section, the behavior of the cost function $Q(\tau)$ is studied for two multipath channel models. It is also shown that for single path channels, the ML-TOA estimator is unbiased and the estimation error variance is inversely proportional to the bandwidth.

Consider first the extreme case in which there is only a direct path at $\tau_0 = 0$ and no additive noise. We have $\mathbf{h} = a\mathbf{1}$ where a is the random path gain. Then, it is easily seen that $\mathbf{K}_{\mathbf{h}} = \sigma_a^2\mathbf{1}\mathbf{1}^T$ where σ_a^2 is the variance of a, then $\mathbf{R} = \sigma_a\mathbf{1}$, $\mathbf{F} = c\mathbf{1}\mathbf{1}^T$ and $\mathbf{y} = \mathbf{h} = a\mathbf{1}$, and the cost function (5) becomes $Q(\tau) = \alpha|\mathbf{1}^T\mathbf{G}\mathbf{1}|^2 = \beta\left(\frac{\sin(\frac{N\pi}{T}\tau)}{\sin(\frac{\pi}{T}\tau)}\right)^2$ where α, β are some constants. The width of the main lobe is inversely proportional to the number of subcarriers N or equivalently the bandwidth. In Figure 1, one realization of the noise free cost function $Q(\tau)$ in a single path channel is shown for the 802.11a configuration where $N = 64$ (see Section 5). It can be seen that it closely matches the theoretical curve where the training sequence is assumed to be all 1's.

In the case of multipath, we first investigate the cost function $Q(\tau)$ when noise is absent. In Figure 2, one realization of the noise free cost function for Exponential channel model and WLAN channel model A (see Section 5 for detailed description of the channel models used in this article) are plotted. Note the noise free cost function for the Exponential channel is fairly flat. As demonstrated in Section 3.1 if $\mathbf{K}_{\mathbf{h}}$ is perfectly known the actual peak of the cost function is at zero offset, but at high SNR, where the flattening effect is observed, an error in $\mathbf{K}_{\mathbf{h}}$ can result in biased TOA estimation (see Figure 3). The noise free cost function for WLAN channel model A shows that a clear peak is present thus is more robust to the error from the estimated channel covariance matrix at high SNR region (see Figure 4). For all other WLAN channel models, i.e., B to D, we have observed that the cost functions have similar characteristics to those for channel model A.

4 ML direct positioning method

In this section, we develop a ML direct estimation of the MS position, (x, y), based on the received FFT vectors from several APs. The proposed ML direct location estimation is shown to provide the correct, unambiguous location in the absence of noise given the channel statistics.

Conventionally, the positioning problem is solved via an indirect (two-step) parameter estmation scheme. First, TOA estimation at each AP is performed. Then, these TOA estimates are transmitted to a central terminal at which the location estimation is carried out. It is sometimes assumed that the TOA estimates in the first step are zero mean Gaussian random variables and then, based on this assumption, the second step applies a least square procedure, which in this case is also a ML estimator, to estimate the position of MS [23-25]. However, it is known that in multipath environments, the TOA estimation can be biased and the estimation error is not Gaussian in practice [25-27]. For these reasons, we propose a ML direct positioning method, based on the ML-TOA

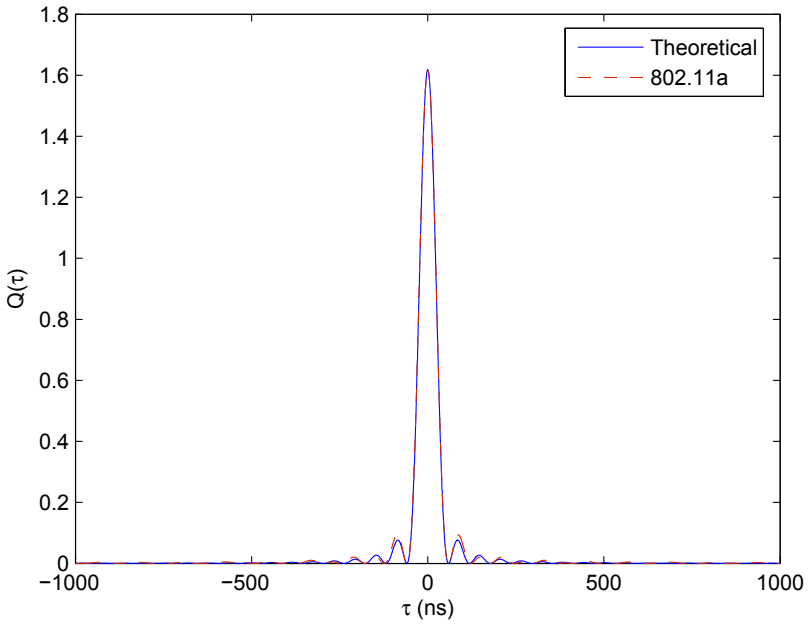

Figure 1 Noise free cost function $Q(\tau)$ for single path channel.

estimator described in Section 2, to estimate the position of MS directly.

For simplicity, in this article, the MS location is assumed to be on a two-dimensional surface, but the derivation can be extended to three dimensions as well. Consider M APs located at height z above the MS with x, y locations (x_i, y_i) $(i = 1, 2,..., M)$ and an MS at an unknown location (x, y). The distance from the MS to the ith AP is then $d_i = \sqrt{(x - x_i)^2 + (y - y_i)^2 + z^2}$. Therefore, the TOA from the MS to the ith AP is $\tau_0^{(i)} = \frac{d_i}{C} = \frac{\sqrt{(x - x_i)^2 + (y - y_i)^2 + z^2}}{C}$, where C is the speed of light. Notice that in this expression, the TOA $\tau_0^{(i)}$ is a function of the unknown position of MS, i.e.,

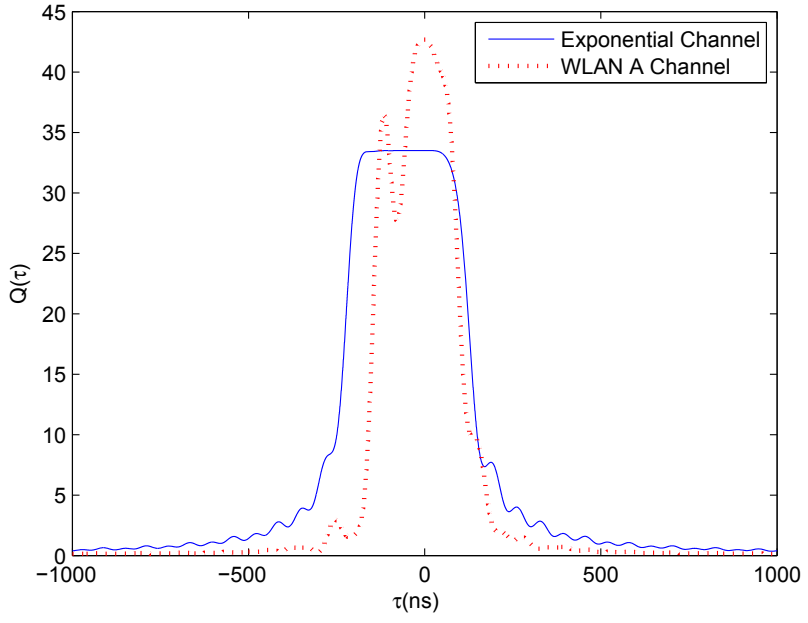

Figure 2 Noise free cost function $Q(\tau)$.

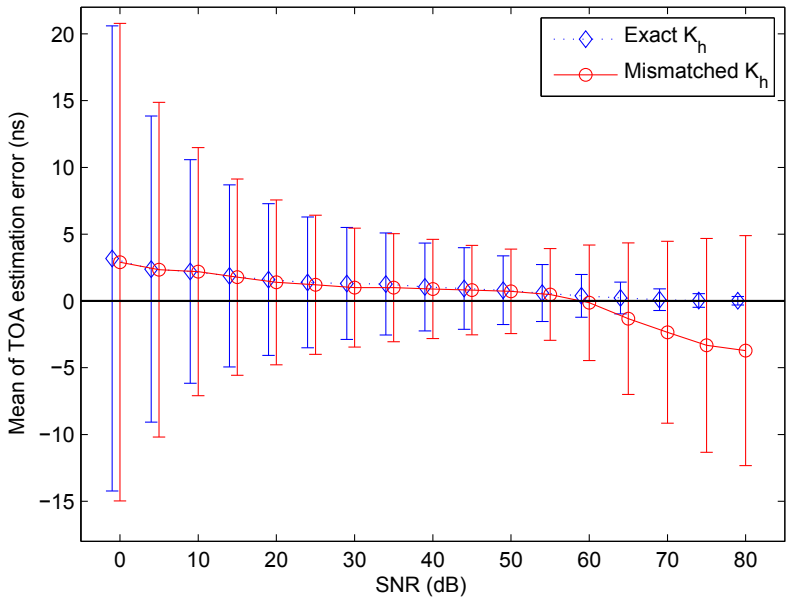

Figure 3 Performance comparisons between estimations using exact and mismatched covariance matrix K_h for the Exponential channel model.

(x, y). We can estimate the position of the MS directly, based on the FFT output vectors at all M APs as follows.

From (3), assuming $\mathbf{D} = \mathbf{I}$, the complete FFT output vector at the ith AP is

$$\mathbf{y}^{(i)} = \mathbf{G}^{(i)}\mathbf{h}^{(i)} + \mathbf{n}^{(i)}, \tag{13}$$

where $\mathbf{G}^{(i)} = \text{diag}\left\{1, e^{-j\frac{2\pi}{CT}\sqrt{(x-x_i)^2+(y-y_i)^2+z^2}}, \ldots, e^{-j(N-1)\frac{2\pi}{CT}\sqrt{(x-x_i)^2+(y-y_i)^2+z^2}}\right\}$. The noise vectors $\mathbf{n}^{(i)}$ are independent, zero mean Gaussian with covariance matrix $\sigma_i^2\mathbf{I}$ and $\mathbf{h}^{(i)}$ is assumed to be a zero mean, circular complex Gaussian vector with known covariance matrix $\mathbf{K}_\mathbf{h}^{(i)} = \mathbb{E}\left\{\mathbf{h}^{(i)}\left(\mathbf{h}^{(i)}\right)^H\right\}$. The

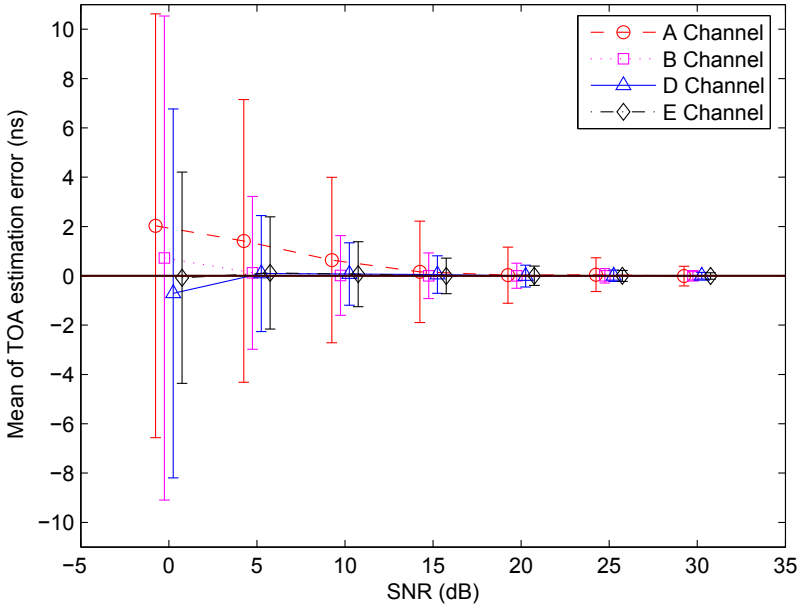

Figure 4 ML TOA performance using WLAN channel models.

channels from the MS to each AP are assumed to be independent. Then, the joint p.d.f. of the received FFT vectors from all APs is

$$p(\mathbf{y}^{(1)}, \mathbf{y}^{(2)}, \ldots, \mathbf{y}^{(M)} | (x,\ y)) = \frac{1}{\pi^{NM} \prod_{i=1}^{M} \mathrm{Det}(\mathbf{K}_{\mathbf{y}}^{(i)})} \exp\left(- \sum_{i=1}^{M} (\mathbf{y}^{(i)})^H (\mathbf{K}_{\mathbf{y}}^{(i)})^{-1} \mathbf{y}^{(i)} \right), \quad (14)$$

where Det(·) denotes the matrix determinant and $\mathbf{K}_{\mathbf{y}}^{(i)} = \mathbb{E}\left\{ \mathbf{y}^{(i)} (\mathbf{y}^{(i)})^H \right\} = \mathbf{G}^{(i)} \mathbf{K}_{\mathbf{h}}^{(i)} (\mathbf{G}^{(i)})^H + \sigma_i^2 \mathbf{I}$. Next, we show the term $\prod_{i=1}^{M} \mathrm{Det}\left(\mathbf{K}_{\mathbf{y}}^{(i)} \right)$ is independent of (x, y). Using the matrix identity, Det $(\mathbf{I} + \mathbf{AB}) = \mathrm{Det}(\mathbf{I} + \mathbf{BA})$, each determinant factor inside the product can be expressed as $\mathrm{Det}\left(\mathbf{K}_{\mathbf{y}}^{(i)} \right) = \sigma_i^{2N} \mathrm{Det}\left(\mathbf{I} + (\mathbf{G}^{(i)})^H \mathbf{G}^{(i)} \mathbf{K}_{\mathbf{h}}^{(i)} / \sigma_i^2 \right)$. Using the fact that $(\mathbf{G}^{(i)})^H \mathbf{G}^{(i)} = \mathbf{I}$, the above determinant becomes $\mathrm{Det}\left(\mathbf{K}_{\mathbf{y}}^{(i)} \right) = \sigma_i^{2N} \mathrm{Det}(\mathbf{I} + \mathbf{K}_{\mathbf{h}}^{(i)} / \sigma_i^2)$ which does not depend on (x, y).

Using (14), the ML solution for (x, y) is given as

$$\begin{aligned} (\hat{x}, \hat{y}) &= \arg\max_{(x,y)} \ln p(\mathbf{y}^{(1)},\ \mathbf{y}^{(2)},\ \ldots,\ \mathbf{y}^{(M)} | (x,\ y)) \\ &= \arg\min_{(x,y)} \sum_{i=1}^{M} (\mathbf{y}^{(i)})^H (\mathbf{K}_{\mathbf{y}}^{(i)})^{-1} \mathbf{y}^{(i)}, \end{aligned} \quad (15)$$

where we use the notation $p\ (\mathbf{y}^{(1)}, \mathbf{y}^{(2)}, ..., \mathbf{y}^{(M)} | (x, y))$ to denote the joint p.d.f. of $\mathbf{y}^{(1)}, \mathbf{y}^{(2)}, ..., \mathbf{y}^{(M)}$ for a generic value (x, y), the location of the MS.

Next, factor $\mathbf{K}_{\mathbf{h}}^{(i)}$ as $\mathbf{K}_{\mathbf{h}}^{(i)} = \mathbf{R}^{(i)} (\mathbf{R}^{(i)})^H$ and using the well-known fact that $(\mathbf{I} + \mathbf{AB})^{-1} = \mathbf{I} - \mathbf{A}(\mathbf{I} + \mathbf{BA})^{-1} \mathbf{B}$, we can write $\left(\mathbf{K}_{\mathbf{y}}^{(i)} \right)^{-1}$ as

$$\left(\mathbf{K}_{\mathbf{y}}^{(i)} \right)^{-1} = \frac{1}{\sigma_i^2} \left[\mathbf{I} - \mathbf{G}^{(i)} \mathbf{R}^{(i)} \left(\sigma_i^2 \mathbf{I} + (\mathbf{R}^{(i)})^H \mathbf{R}^{(i)} \right)^{-1} (\mathbf{R}^{(i)})^H (\mathbf{G}^{(i)})^H \right]. \quad (16)$$

Use this in (15) and define

$$Q^{(i)}(x,\ y) \triangleq \frac{1}{\sigma_i^2} (\mathbf{y}^{(i)})^H \mathbf{G}^{(i)} \mathbf{F}^{(i)} (\mathbf{G}^{(i)})^H \mathbf{y}^{(i)}, \quad (17)$$

where $\mathbf{F}^{(i)} = \mathbf{R}^{(i)} \left[\sigma_i^2 \mathbf{I} + (\mathbf{R}^{(i)})^H \mathbf{R}^{(i)} \right]^{-1} (\mathbf{R}^{(i)})^H$. Then, the ML direct estimation for the MS location (x, y) is

$$(\hat{x}, \hat{y}) = \arg\max_{(x,y)} \sum_{i=1}^{M} Q^{(i)}(x,\ y), \quad (18)$$

where the unknown parameter (x, y) is embedded in $\mathbf{G}^{(i)}$. Note that $\mathbf{F}^{(i)}$ can be computed off-line given σ_i^2 and $\mathbf{K}_{\mathbf{h}}^{(i)}$.

Next, we show that the ML direct positioning estimate based on (18) is unambiguously correct in the absence of noise. Denote (x_0, y_0) and $\tau_0^{(i)}$ the true location of the MS and the true TOA for the ith AP, respectively. From the uniqueness property shown in Section 3.1, it follows that, given i, $Q^{(i)}(\tau^{(i)}) = \frac{1}{\sigma_i^2} (\mathbf{y}^{(i)})^H \mathbf{G}^{(i)} \mathbf{F}^{(i)} (\mathbf{G}^{(i)})^H \mathbf{y}^{(i)}$ is maximized only at $\tau^{(i)} = \tau_0^{(i)} = \frac{\sqrt{(x_0 - x_i)^2 + (y_0 - y_i)^2 + z^2}}{C}$. Assume that the ML direct location estimate is not unique. Then, from (18), there exists $(x, y) \neq (x_0, y_0)$ such that

$$\sum_{i=1}^{M} Q^{(i)}(x,\ y) = \sum_{i=1}^{M} Q^{(i)}(x_0,\ y_0). \quad (19)$$

However, from the uniqueness property, it follows that $Q^{(i)}(x_0,\ y_0) = Q^{(i)}\left(\tau_0^{(i)} \right) > Q^{(i)}\left(\tau^{(i)} \right)$ for all $\tau^{(i)} \neq \tau_0^{(i)}$. Therefore, (19) is true if and only if there exists $(x, y) \neq (x_0, y_0)$ that satisfies $\tau^{(i)} = \tau_0^{(i)}$. In other words, there exist some $(x, y) \neq (x_0, y_0)$ such that the following system of equations are satisfied:

$$\tau_0^{(i)} = \frac{d_i}{C} = \frac{\sqrt{(x - x_i)^2 + (y - y_i)^2 + z^2}}{C}, \quad i = 1, 2, \ldots, M. \quad (20)$$

However, by the trilateration principle that is commonly used in positioning, this cannot be true when $M \geq 3$ and thus a contradiction. Therefore, the proposed ML direct position estimate is unique.

5 Simulation results

The wireless system simulated here is based on the IEEE 802.11a standard [28]. The long training sequence is used for localization. The simulation parameters of the transmitted OFDM signal are: BW = 20 MHz, N = 64 subcarriers are used, T = 3.2 and T_G = 1.6 μs. Two periods of the long sequence are transmitted to improved channel estimation accuracy, yielding the total duration of the long training sequence, $T_G + 2T$ = 8 μs. Two channel models are used in the simulations. One is the Exponential channel model similar to the ones used in [13,29] and the other is the WLAN channel model [30]. The power delay profiles for the five WLAN channels are shown in Table 1. The root-mean-square (RMS) delays for channels A through E are 50, 100, 150, 140 and 250 ns, respectively. The Exponential channel is generated assuming the path delays represent a Poisson process with average time between points equal to t_{int} and an Exponential power delay profile with the RMS amplitudes decaying by the fraction ρ over a $t_{\max}$ delay spread. In the simulations, the parameters for Exponential channels are chosen to be t_{int} = 10 ns, $t_{\max}$ = 200 ns and decay ρ = 0.003. With these parameters, there are on average 20 paths in total and the power decay is -2.5

Table 1 Power delay profiles for the WLAN channels

Model A Delay (ns)	0	10	20	30	40	50	60	70	80	90	110	140	170	200	240	290	340	390
Power (dB)	0	-0.9	-1.7	-2.6	-3.5	-4.3	-5.2	-6.1	-6.9	-7.8	-4.7	-7.3	-9.9	-12.5	-13.7	-18	-22.4	-26.7
Model B Delay (ns)	0	10	20	30	50	80	110	140	180	230	280	330	380	430	490	560	640	730
Power (dB)	-2.6	-3.0	-3.5	-3.9	0	-1.3	-2.6	-3.9	-3.4	-5.6	-7.7	-9.9	-12.1	-14.3	-15.4	-18.4	-20.7	-24.6
Model C Delay (ns)	0	10	20	30	50	80	110	140	180	230	280	330	400	490	600	730	880	1050
Power (dB)	-3.3	-3.6	-3.9	-4.2	0	-0.9	-1.7	-2.6	-1.5	-3.0	-4.4	-5.9	-5.3	-7.9	-9.4	-13.2	-16.3	-21.2
Model D Delay (ns)	0	10	20	30	50	80	110	140	180	230	280	330	400	490	600	730	880	1050
Power (dB)	0	-10	-10.3	-10.6	-6.4	-7.2	-8.1	-9.0	-7.9	-9.4	-10.8	-12.3	-11.7	-14.3	-15.8	-19.6	-22.7	-27.6
Model E Delay (ns)	0	10	20	40	70	100	140	190	240	320	430	560	710	880	1070	1280	1510	1760
Power (dB)	-4.9	-5.1	-5.2	-0.8	-1.3	-1.9	-0.3	-1.2	-2.1	0	-1.9	-2.8	-5.4	-7.3	-10.6	-13.4	-17.4	-20.9

dB for each path. The channel covariance matrix $\hat{\mathbf{K}}_{\mathbf{h}}$ is estimated using the procedures described in Section 3.2 with 100 samples and 40 dB received signal SNR. The received SNR is defined as, assuming the transmit signal power is unity, $\text{SNR} \triangleq \frac{\mathbb{E}\{\Sigma_{i=0}^{L-1}|a_i^2|\}}{\sigma^2}$.

5.1 Performance of the ML-TOA estimator

The performance of the ML-TOA estimator described in Section 2 has been thoroughly presented in [10] in the case when there is a significant LOS path present. In this section, we first discuss its performance in NLOS channels and then consider the effects of matched vs. mismatched statistics. As discussed in Section 3.2, the ML-TOA estimation procedure takes the statistics of NLOS channels into account automatically. Recall that the term "NLOS delay" refers to the time difference between the first arriving path delay and the TOA as defined in Section 3.2. If a direct LOS path exists, the NLOS delay is zero. Gaussian and Exponential distributions are assumed for the NLOS delay in the simulations [31,32]. In Figure 5, the NLOS delay is assumed to be Gaussian with mean 15 ns and variance 10 or Exponential with mean β = 3 ns. The bottom curve (LOS/LOS $\mathbf{K}_{\mathbf{h}}$) is the performance when the LOS path exists. The curves (NLOS/NLOS $\mathbf{K}_{\mathbf{h}}$) are the situations when the channel contains no LOS path. The curves (NLOS/LOS $\mathbf{K}_{\mathbf{h}}$) serve as references and they represent a NLOS case but when estimating $\hat{\mathbf{K}}_{\mathbf{h}}$, $\tau_0^{(i)}$ is chosen to equal the first arriving path delay instead of the TOA. The figure shows that the NLOS performance is comparable to that of the LOS case when channel measurements are made in the same NLOS scenario. If the LOS covariance matrix is used in the NLOS case (NLOS/LOS $\mathbf{K}_{\mathbf{h}}$), however, an increased bias is seen.

Next, we compare the performance of the ML-TOA estimator when the Exponential channel model is used vs. when the WLAN channel models are used, and also discuss the dependence of its performance on the number of samples used in estimating the covariance matrix. The error-bar plot is used in Figures 3 and 4. The center of the error bar is the mean of the estimation error and the length of the bar equals twice the standard deviation. In order to make it easier to distinguish different curves in the error-bar plot, they are off-set in the horizontal axis deliberately. These statistics are computed after 10, 000 trials. Figure 3 shows the performance of the ML-TOA estimator for the Exponential channel in the case where a LOS path exists. In order to show the robustness of the ML-TOA estimator, we compare the cases of mismatched and matched statistics. In the mismatched case, which corresponds to the practical application, the estimated covariance matrix $\hat{\mathbf{K}}_{\mathbf{h}}$ is measured as in Section 3.2 using 100 averaged samples. For the matched covariance matrix case, the channel is generated by $\mathbf{h} = \mathbf{Rz}$ to ensure that its covariance matrix is strictly equal to $\mathbf{K}_{\mathbf{h}}$. From Figure 3, we can see that in the SNR range 0-40 dB, the estimation error $\Delta\mathbf{K}_{\mathbf{h}}$ does not cause much performance degradation for the Exponential channel. At high SNR region, as discussed in Section 3.3, due to the flattening of the cost function, $\Delta\mathbf{K}_{\mathbf{h}}$ results in biased estimates. From the performance of the matched case, it is seen indirectly that the cost function has a unique maximizer, for at high SNR, the estimation is unbiased and the variance is zero.

For the WLAN channel models, Figure 4 shows the performance for different channel types. By comparing Figure 4 with Figure 3, it seems that the performance for the WLAN channel models is slightly better than for the Exponential channels. This is related to the fact that, for these channels, the cost function has clear peak (see Figure 2). Channel type A yields worst performance among the WLAN channels, which may be due to the fact that its power delay profile is most similar to an Exponential channel which has a flat noise free cost function.

Figure 6 shows the performance of the WLAN channel A as the number of samples used for estimating $\mathbf{K}_{\mathbf{h}}$ is varied. Since $\hat{\mathbf{K}}_{\mathbf{h}}$ is a random quantity for any given number of samples, we use the following process in generating this figure. When the number of samples is P, $\hat{\mathbf{K}}_{\mathbf{h}}$ is estimated using P averaged random channels (MS

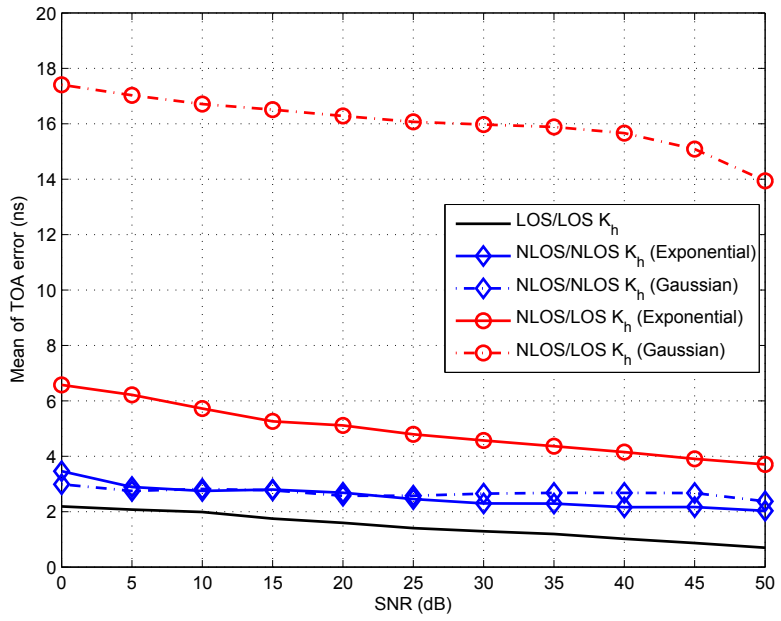

Figure 5 LOS and NLOS TOA performance comparisons.

locations) with SNR at 40 dB. Next, using this specific $\hat{\mathbf{K}}_\mathbf{h}$, 100 random ML-TOA estimation trials are performed for each SNR value and the errors are recorded. Next, a new $\hat{\mathbf{K}}_\mathbf{h}$ is generated using another P averaged samples, and another 100 random ML-TOA estimation trials are performed for each SNR value. This is repeated for 10 different estimated $\hat{\mathbf{K}}_\mathbf{h}$ matrices, for a total of 1, 000 TOA estimation error values, and the statistics are then plotted to yield the curves in Figure 6. Figures 7 and 8 show the corresponding results for the WLAN channel D and Exponential channel. As one would expect, there is some fluctuation in the curves, which decreases with increasing P, but for $P \geq 100$ the curves track each other fairly closely. For the remainder of the article, $P = 100$ is used in the simulations presented.

Table 2 presents some error statistics for $\mathbf{K}_\mathbf{h}$ itself. For each value of P (number of averaged samples) the table shows the maximum (over all elements of $\hat{\mathbf{K}}_\mathbf{h}$) of the normalized RMS error in the elements of $\hat{\mathbf{K}}_\mathbf{h}$ over 1, 000 random estimates. The error is the difference between $\hat{\mathbf{K}}_\mathbf{h}$ and the "true" covariance matrix as estimated using 10, 000 samples. Then, the normalization is obtained by dividing the RMS error in each element by the magnitude of the "true" covariance matrix. In practice, for a given indoor environment, an initial estimation of $\mathbf{K}_\mathbf{h}$ would be carried out off-line prior to the employment of the ML-TOA procedure for localization. Subsequent additional measurements for this purpose could then be added later to improve the estimation accuracy if necessary.

5.2 Performance of ML direct positioning

We compare the performance of two localization schemes. One is the proposed ML direct location technique discussed in Section 4. The other is an indirect (two-step) method which first uses the ML-TOA estimation approach described in Section 2 for TOA estimates then least square localization solvers described in [3], namely the TOA-least square (TOA-LS) and TOA-weighted constraint LS (TOA-WCLS) techniques, are adopted to solve for the location of the MS. The least square localization solvers can be used with any TOA estimation technique for the individual AP's, but here we use the ML-TOA estimation approach described in Section 2 so that both techniques have the benefit of the measured channel statistics. A five AP geometry is considered in a 100 m × 100 m square with AP coordinates; (5, 10), (50, 50), (80, 20), (10, 75) and (90, 90), respectively. We show results for three MS locations, namely at (x, y) = (20, 20), (20, 90) and (70, 70). The channel impulse responses for each of the five APs are generated randomly using the aforementioned channel models.

In the simulations, the average SNR is defined as $\frac{1}{M}\sum_{i=1}^{M} \mathrm{SNR}_i$, where SNR_i is the signal-to-noise power ratio at the ith AP. The path loss exponent is assumed to be 3 for indoor environments. The weighting matrix $\mathbf{W}$ used in TOA-WCLS is then chosen such that the

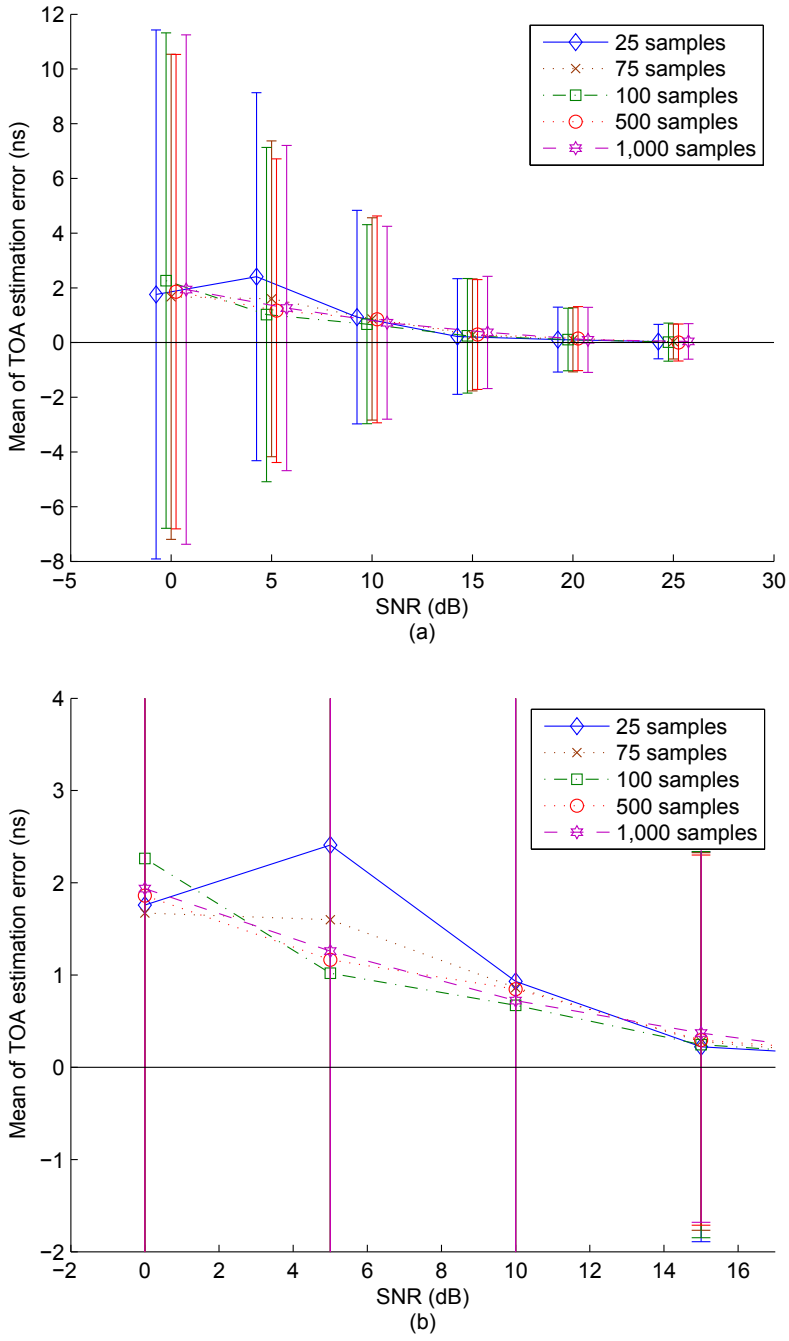

Figure 6 WLAN channel A: (a) TOA estimation error with respect to number of averaged samples for K_h; (b) expanded scale.

diagonal elements are $w_{ii} = \frac{\mathrm{SNR}_i}{\Sigma_{i=1}^{M} \mathrm{SNR}_i}$. The results shown here are obtained by running 10,000 random trials.

Figures 9 through 12 are for MS location at $(x, y) = (20, 20)$. Figures 9 and 10 show the performance comparisons between the direct method and the indirect (TOA-LS and TOA-WCLS) methods for the Exponential channel models. Figure 9 shows the 90% percentage error values versus average SNR. The 90% percentage error value is the value such that 90% of all errors are less than that value. As expected, the direct method outperforms the TOA-LS and TOA-WCLS methods, and the TOA-WCLS performs better than the TOA-LS, which imposes no weighting constraint. For the Exponential channel model, it is seen that due to the bias of the TOA estimations, the direct and indirect methods

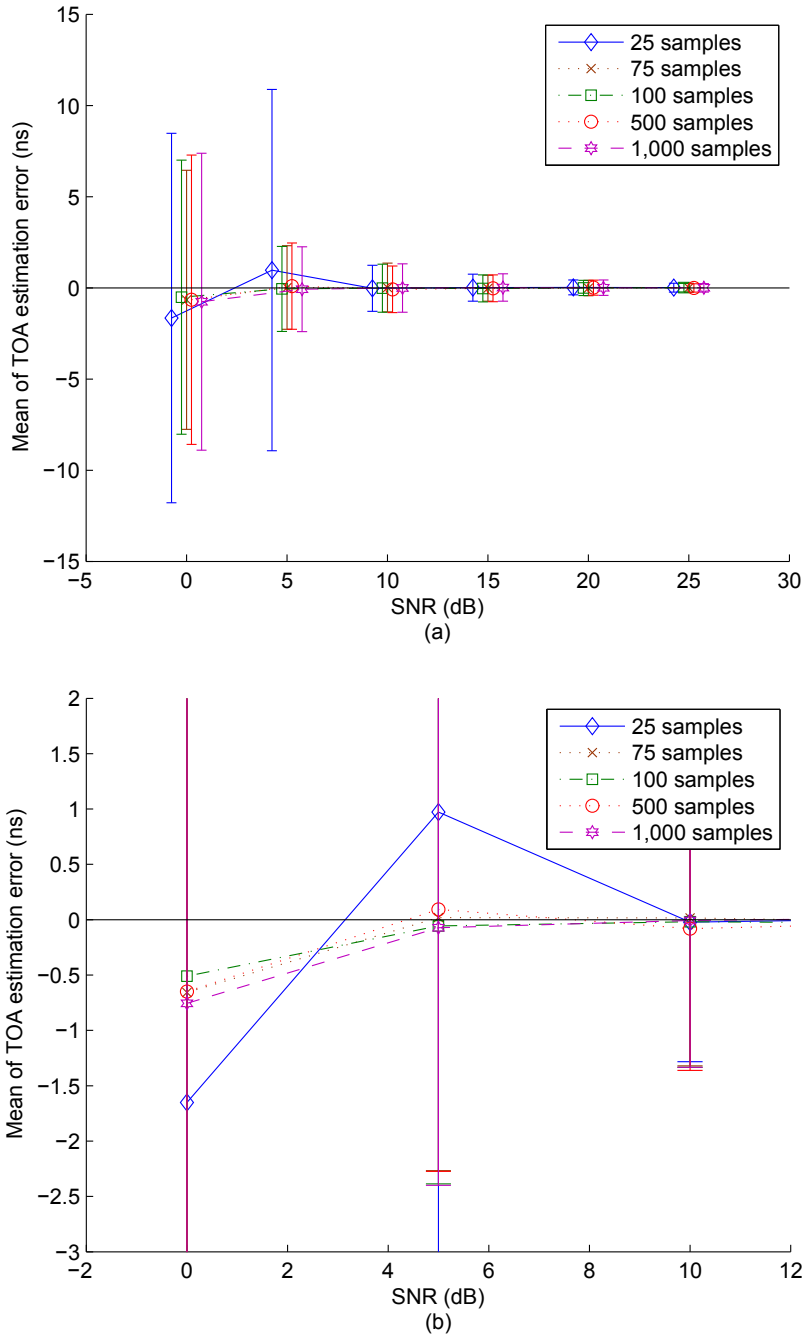

Figure 7 WLAN channel D: (a) TOA estimation error with respect to number of averaged samples for K_h; (b) expanded scale.

do not converge at high SNR, with the direct method maintaining its superiority. This is one rationale behind using the direct method. Figure 10 shows the mean square error (MSE) of the direct and indirect methods. Again, it is seen that the direct method has the best performance. Figures 11 and 12 show the performance with WLAN channel models A and D. Since the ML-TOA estimates of WLAN channels are unbiased when SNR is high (see Figure 4), we do not show the performance at very high SNR for the performance converges. Figure 12 illustrates the CRLB as a performance reference for the WLAN channels. The CRLB is a lower bound on the variance of any unbiased estimator. Thus, we show it as a performance reference for the WLAN channels. The expressions for the CRLB can be found in Appendix A (due to limited space the detailed derivation is omitted).

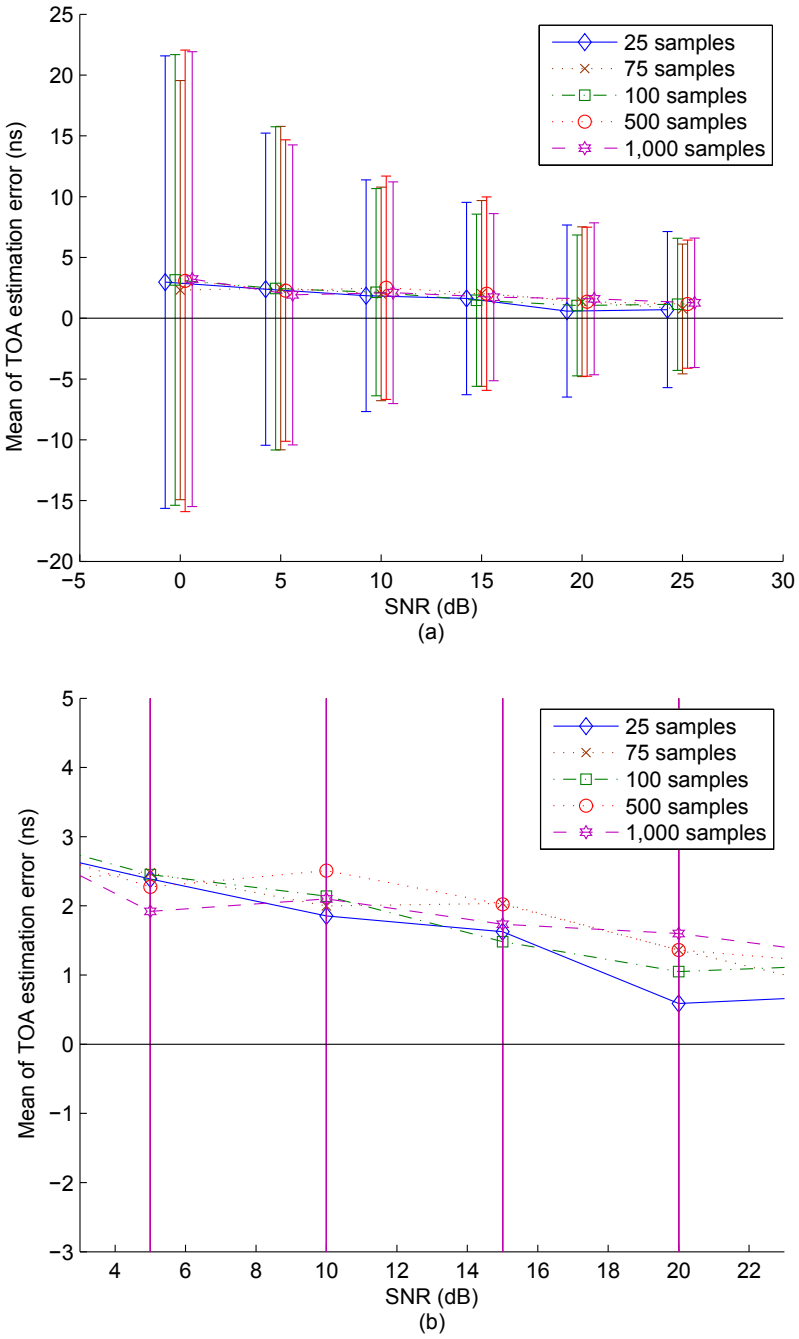

Figure 8 Exponential channel: (a) TOA estimation error with respect to number of averaged samples for K_h; (b) expanded scale.

Table 2 K_h estimation error statistics

Samples	Max. normalized RMS error
25	1.422×10^{-2}
100	3.347×10^{-3}
500	2.614×10^{-3}
1, 000	2.302×10^{-3}

When computing the CRLB, each estimated channel covariance matrix $\mathbf{K}_{\mathbf{h}}^{(i)}$ is obtained by time-averaging 10, 000 random generated channels. The direct method again shows the best performance. Furthermore, the ML direct method is shown to have performance close to the CRLB. One can see that the performance for the

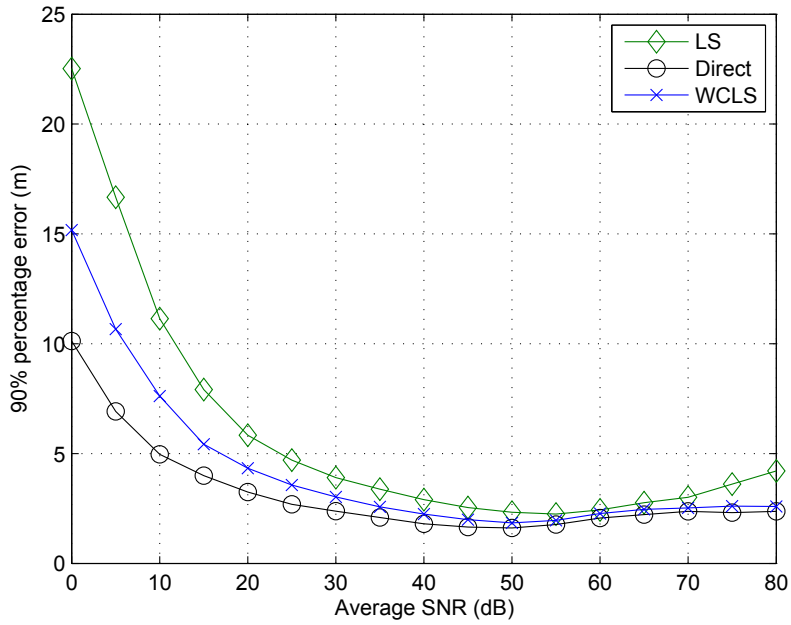

Figure 9 90% percentage error for direct and indirect (two-stage) methods using Exponential channel model.

WLAN model is better than for the Exponential model due to biased ML-TOA estimates in the latter. Figures 13 and 14 show the performance comparisons in WLAN channel model A for MS at (20, 90) and (70, 70). These two figures show results consistent with Figures 11 and 12.

6 Conclusions

Several important results regarding the ML-TOA estimator for dense multipath indoor channels have been established. First, the unambiguous accuracy of the ML-TOA solution is proved in the noise free case, when multipath is the only detrimental effect of the channel.

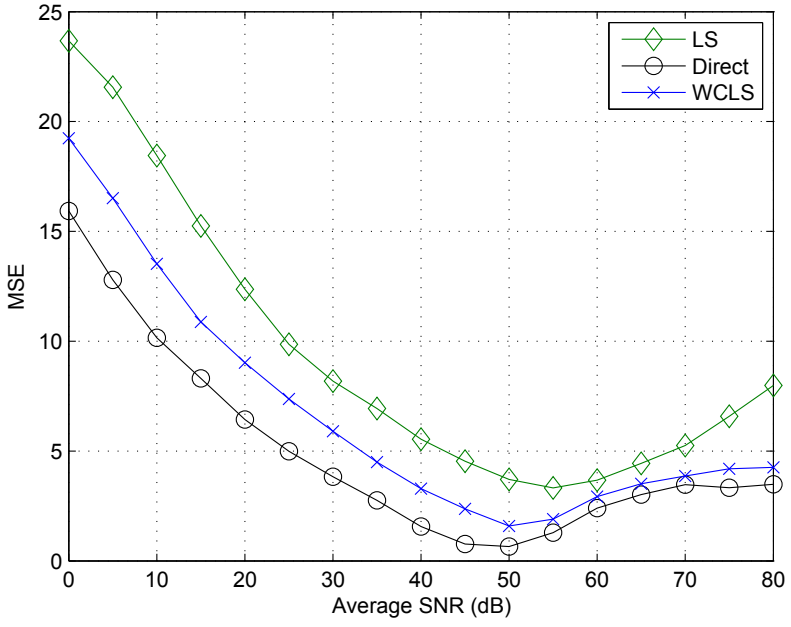

Figure 10 Mean square error (MSE) in dB scale for direct and indirect (two-stage) methods using Exponential channel model.

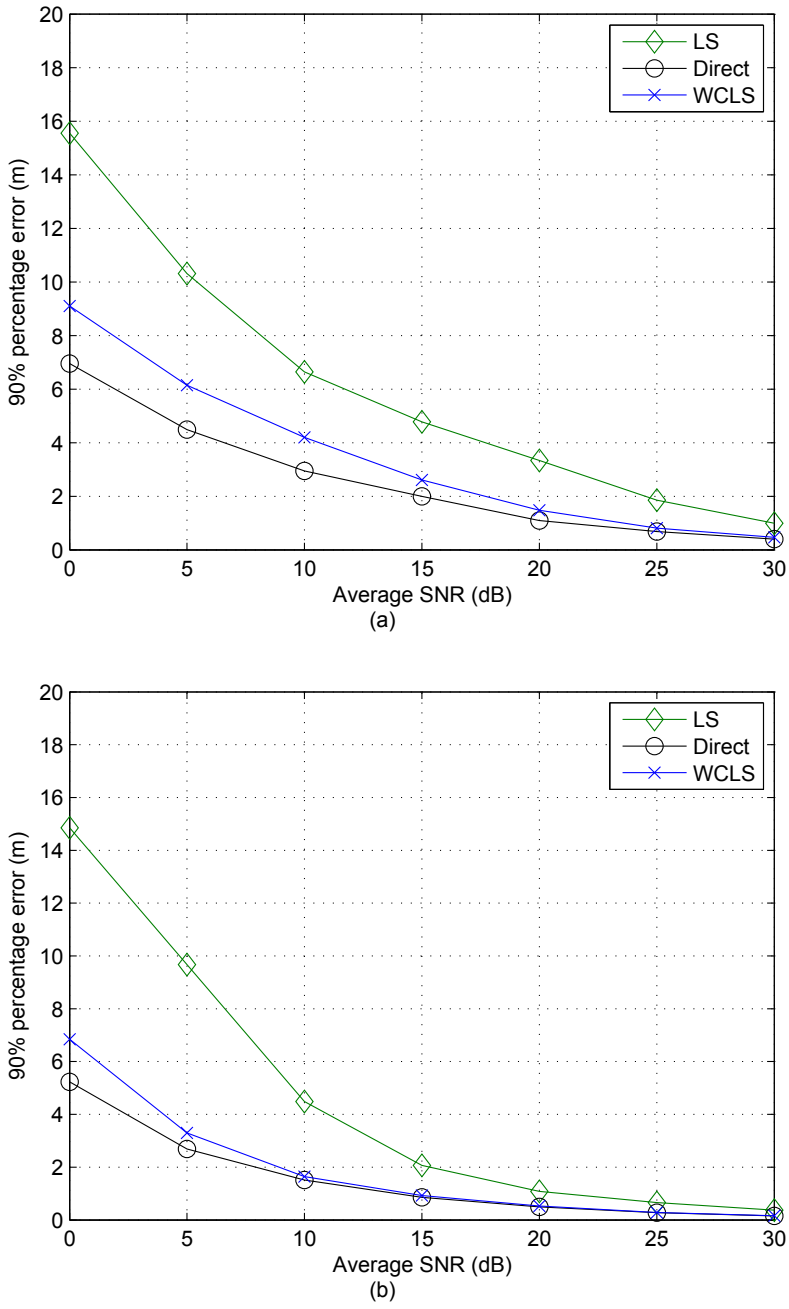

Figure 11 90% percentage error for direct and indirect (two-stage) methods: (a) WLAN channel model A; (b) WLAN channel model D.

Then, the behavior in the NLOS case was discussed. Because of its statistical basis, the ML-TOA technique automatically incorporates the NLOS case in which there does not actually exist a direct path from the AP to the MS. The performance of the ML-TOA estimator was also detailed. It was shown that for single path channels, the ML-TOA estimator is unbiased and the estimation error variance is inversely proportional to the bandwidth. For multipath channels, the error is dependent upon the specific characteristics of the channels. Finally, we have shown how to extend the statistical channel model (ML-TOA) approach to a direct ML localization technique which enables us to obtain a ML estimator that directly estimates the location of the MS. Results were compared to an indirect approach in which TOA estimates are obtained by the ML-TOA estimator and a least squares technique is then used to localize the MS. The direct ML location estimation is shown to

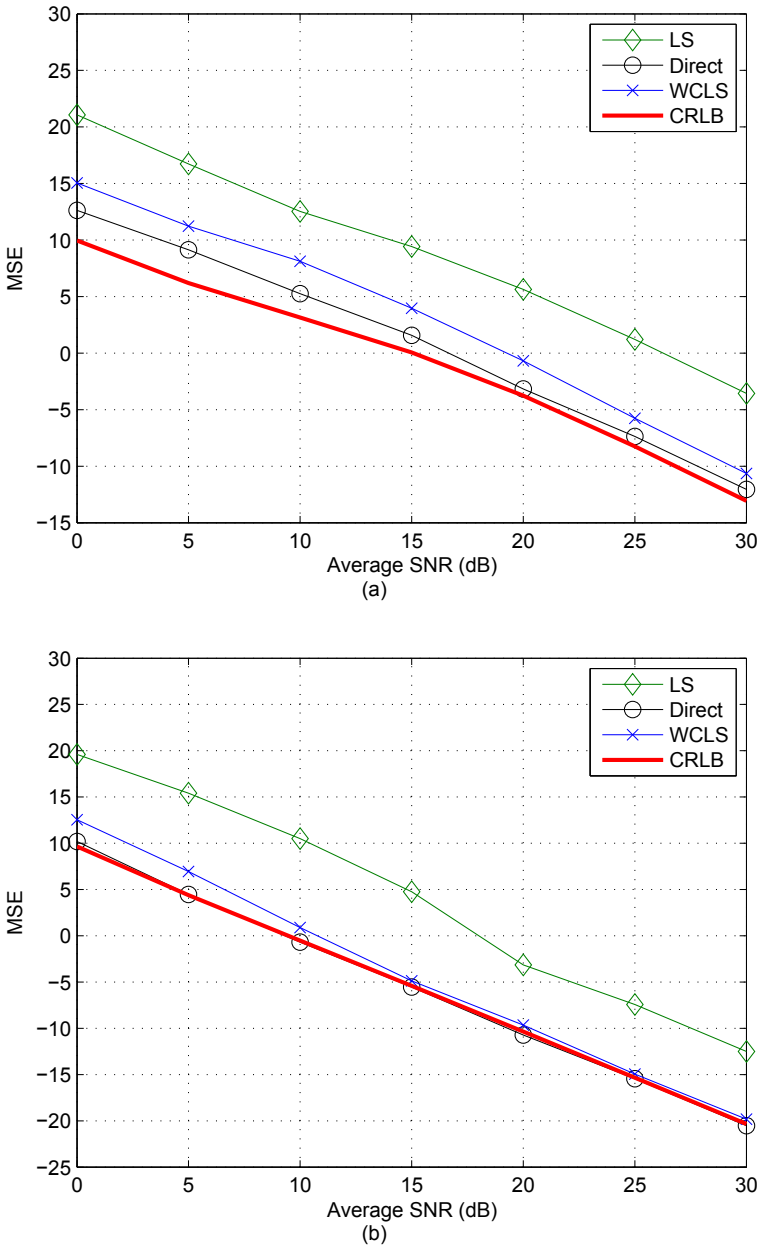

Figure 12 Mean square error (MSE) in dB scale for direct and indirect (two-stage) methods: (a) WLAN channel model A; (b) WLAN channel model D.

outperform the indirect methods and obtain performance close to the CRLB for some channel types.

Appendix A: Cramer-Rao lower bound for the ML direct position estimator

For the position estimation problem in which the unknown parameter is $\mathbf{u} = [x\ y]^T$, Fisher's Information Matrix [33] is given by

$$\mathbf{I}(\mathbf{u}) = -\begin{bmatrix} \mathbb{E}\left\{\frac{\partial^2 \ln p(\mathbf{y}|\mathbf{u})}{\partial x^2}\right\} & \mathbb{E}\left\{\frac{\partial^2 \ln p(\mathbf{y}|\mathbf{u})}{\partial x \partial y}\right\} \\ \mathbb{E}\left\{\frac{\partial^2 \ln p(\mathbf{y}|\mathbf{u})}{\partial y \partial x}\right\} & \mathbb{E}\left\{\frac{\partial^2 \ln p(\mathbf{y}|\mathbf{u})}{\partial y^2}\right\} \end{bmatrix}.$$

From (14) and the well-known identity tr(**AB**) = tr(**BA**), the elements of the Fisher's information matrix are given by

$$\mathbb{E}\left\{\frac{\partial^2 \ln p(\mathbf{y}|\mathbf{u})}{\partial x^2}\right\} = \sum_{i=1}^{M} \frac{2}{\sigma_i^2} \mathrm{Re}\left\{\mathrm{tr}\left[\left(\mathbf{D}_c^{(i)}\mathbf{C}_{\mathbf{R}}^{(i)} + (\mathbf{D}_x^{(i)})^2\mathbf{C}_{\mathbf{R}}^{(i)} + \mathbf{D}_x^{(i)}\mathbf{C}_{\mathbf{R}}^{(i)}(\mathbf{D}_x^{(i)})^H\right)\mathbf{K}_{\mathbf{y}}^{(i)}\right]\right\}, \quad (21)$$

$$\mathbb{E}\left\{\frac{\partial^2 \ln p(\mathbf{y}|\mathbf{u})}{\partial y^2}\right\} = \sum_{i=1}^{M} \frac{2}{\sigma_i^2} \mathrm{Re}\left\{\mathrm{tr}\left[\left(\mathbf{D}_c^{(i)}\mathbf{C}_{\mathbf{R}}^{(i)} + (\mathbf{D}_y^{(i)})^2\mathbf{C}_{\mathbf{R}}^{(i)} + \mathbf{D}_y^{(i)}\mathbf{C}_{\mathbf{R}}^{(i)}(\mathbf{D}_y^{(i)})^H\right)\mathbf{K}_{\mathbf{y}}^{(i)}\right]\right\} \quad (22)$$

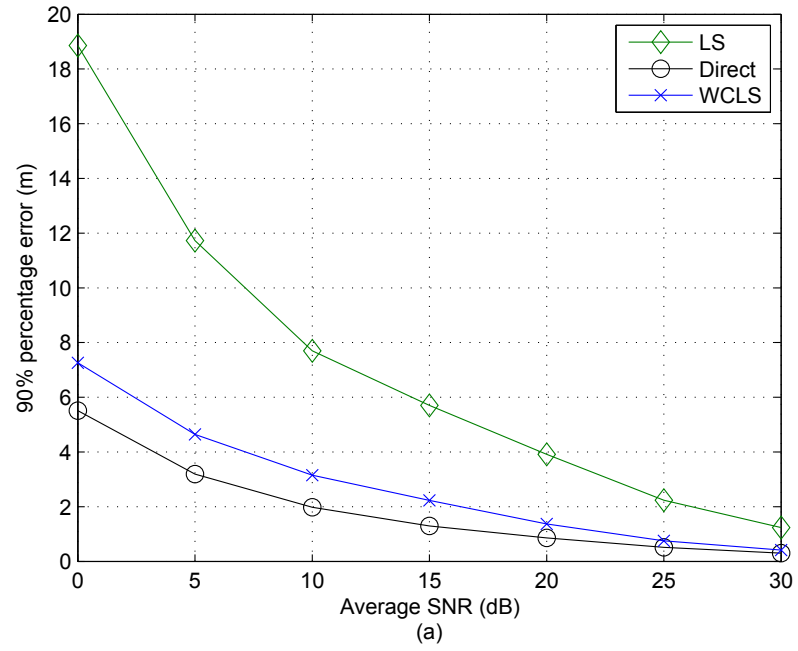

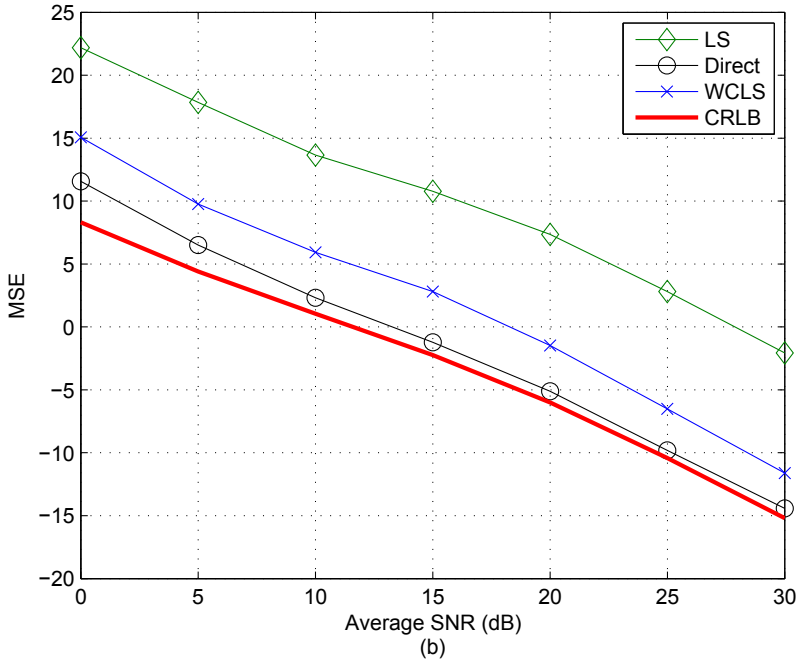

Figure 13 Location error comparisons for MS at (*x*, *y*) = (20, 90) in WLAN channel model A: (a) 90% percentage error; (b) mean square error (MSE).

and

$$\mathbb{E}\left\{\frac{\partial^2 \ln p(\mathbf{y}|\mathbf{u})}{\partial x \partial y}\right\} = \sum_{i=1}^{M} \frac{2}{\sigma_i^2} \mathrm{Re}\left\{\mathrm{tr}\left[\left(\mathbf{D}_{xy}^{(i)}\mathbf{C}_{\mathbf{R}}^{(i)} + \mathbf{D}_{x}^{(i)}\mathbf{C}_{\mathbf{R}}^{(i)}\left(\mathbf{D}_{y}^{(i)}\right)^{H}\right)\mathbf{K}_{\mathbf{y}}^{(i)}\right]\right\}, \quad (23)$$

where $\mathbf{D}_x^{(i)} = \mathrm{diag}\left\{0, -j\frac{2\pi(x-x_i)}{Cd_iT}, -2j\frac{2\pi(x-x_i)}{Cd_iT}, \ldots, -(N-1)j\frac{2\pi(x-x_i)}{Cd_iT}\right\}$,

$\mathbf{D}_y^{(i)} = \mathrm{diag}\left\{0, -j\frac{2\pi(y-y_i)}{Cd_iT}, -2j\frac{2\pi(y-y_i)}{Cd_iT}, \ldots, -(N-1)j\frac{2\pi(y-y_i)}{Cd_iT}\right\}$,

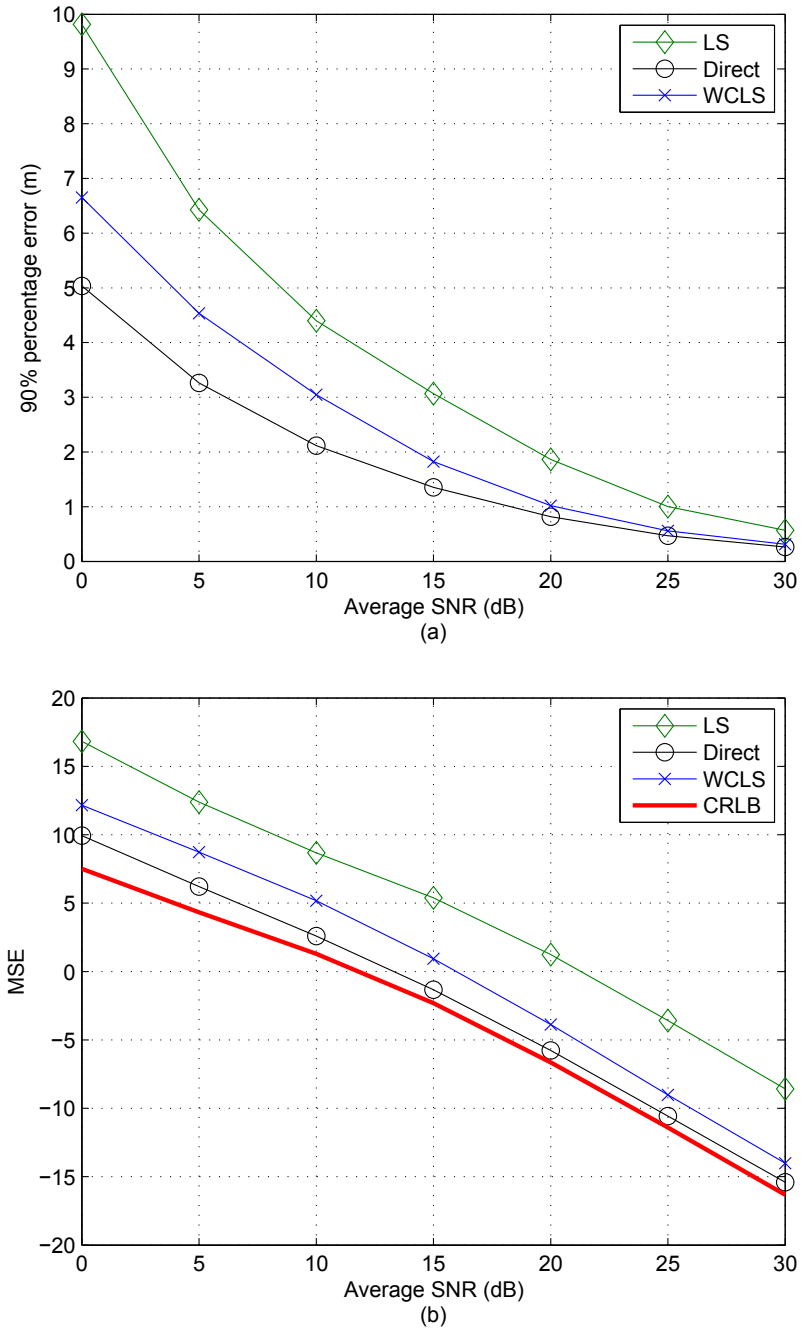

Figure 14 Location error comparisons for MS at (*x*, *y*) = (70, 70) in WLAN model channel A: (a) 90% percentage error; (b) mean square error (MSE).

$$\mathbf{D}_{\epsilon}^{(i)} = \text{diag}\left\{0, -j\frac{2\pi}{Cd_iT}, -j2\frac{2\pi}{Cd_iT}, \ldots, -j(N-1)\frac{2\pi}{Cd_iT}\right\}, \mathbf{D}_{xy}^{(i)} = \mathbf{D}_{x}^{(i)}\mathbf{D}_{y}^{(i)}, \mathbf{C}_{\mathbf{R}}^{(i)} = \mathbf{G}^{(i)}\mathbf{F}^{(i)}(\mathbf{G}^{(i)})^{H}$$

and Re (·) denotes the real part of the argument.

Author details
[1]ITRI (Industrial Technology Research Institute), 195, Sec. 4, Chung Hsing Rd., Chutung, Hsinchu 310, Taiwan [2]Electrical and Computer Engineering Department, Polytechnic Institute of New York University, Six MetroTech Center, Brooklyn, NY 11201, USA

Competing interests
The authors declare that they have no competing interests.

Received: 17 February 2011 Accepted: 30 November 2011
Published: 30 November 2011

References

1. A Smailagic, D Kogan, Location sensing and privacy in a context-aware computing environment. IEEE Commun Mag. **9**(5), 10–17 (2002). doi:10.1109/MWC.2002.1043849
2. J Caffery, GL Stuber, Subscriber location in CDMA cellular networks. IEEE Trans Veh Technol. **47**(2), 406–416 (1998). doi:10.1109/25.669079
3. K Cheung, H So, W-K Ma, Y Chan, Least squares algorithms for time-of-arrival-based mobile location. IEEE Trans Signal Process. **52**(4), 1121–1130 (2004). doi:10.1109/TSP.2004.823465
4. AJ Weiss, Direct position determination of narrowband radio frequency transmitters. IEEE Signal Process Lett. **11**(5), 513–516 (2004). doi:10.1109/LSP.2004.826501
5. F-X Ge, D Shen, Y Peng, V Li, Super-resolution time delay estimation in multipath environments. IEEE Trans Circuits Syst I. **54**(9), 1977–1986 (2007)
6. P Stoica, N Arye, MUSIC, maximum likelihood, and Cramer-Rao bound. IEEE Trans Acoust Speech Signal Process. **37**(5), 720–741 (1998)
7. H Saarnisaari, TLS-ESPRIT in a time delay estimation, in *Proceedings of the IEEE Vehicular Technology Conference*, 1619–1623 (1998)
8. R Wu, J Li, Z-S Liu, Super resolution time delay estimation via MODE-WRELAX. IEEE Trans Aerosp Electron Syst. **35**(1), 207–304 (1999)
9. X Li, K Pahlavan, Super-resolution TOA estimation with diversity for indoor geolocation. IEEE Trans. Wireless Commun. **3**(1), 224–234 (2004). doi:10.1109/TWC.2003.819035
10. P Voltz, D Hernandez, Maximum likelihood time of arrival estimation for real-time physical location tracking of 802.11a/g mobile stations in indoor environments, in *Proceedings of the IEEE Position, Location and Navigation Symposium*, 585–591 (2004)
11. R Kumaresan, AK Shaw, High resolution bearing estimation without eigen decomposition, in *Proceedings of the IEEE International Conference on Acoustics, Speech, and Signal Processing*, 576–579 (1985)
12. Y Bresler, A Macovski, Exact maximum likelihood parameter estimation of superimposed exponential signals in noise. IEEE Trans Acoust Speech Signal Process. **34**(5), 1081–1089 (1986). doi:10.1109/TASSP.1986.1164949
13. Y Qi, H Kobayashi, H Suda, On time-of-arrival positioning in a multipath environment. IEEE Trans Veh Technol. **55**(5), 1516–1526 (2006). doi:10.1109/TVT.2006.878566
14. B Denis, J Keignart, N Daniele, Impact of NLOS propagation upon ranging precision in UWB systems, in *Proceedings of the IEEE Conference on Ultra Wideband Systems Technologies*, 379–383 (2003)
15. W Kim, JG Lee, G-I Jee, The interior-point method for an optimal treatment of bias in trilateration location. IEEE Trans Veh Technol. **55**(4), 1291–1301 (2006). doi:10.1109/TVT.2006.877760
16. K Yu, YJ Guo, Improved positioning algorithms for nonline-of-sight environments. IEEE Trans Veh Technol. **57**(4), 2342–2353 (2008)
17. S Al-Jazzar, J Caffery, H You, A scattering model based approach to NLOS mitigation in TOA location systems, in *Proceedings of the IEEE Vehicular Technology Conference*, 861–865 (2002)
18. P Chen, A nonline-of-sight error mitigation algorithm in location estimation, in *Proceedings of the IEEE Wireless Communications and Networking Conference*, 316–320 (1999)
19. O Bar-Shalom, AJ Weiss, A direct position determination of OFDM signals, in *Proceedings of the IEEE International Workshop on Signal Processing Advances in Wireless Communications*, 1–5 (2007)
20. A Gorokhov, J-P Linnartz, Robust OFDM receivers for dispersive time-varying channels: equalization and channel acquisition, in *IEEE Trans Commun.* **52**(4), 572–583 (2004). doi:10.1109/TCOMM.2004.826354
21. JP Ianniello, Large and small error performance limits for multipath time estimation. IEEE Trans Acoust Speech Signal Process. **34**(2), 245–251 (1986). doi:10.1109/TASSP.1986.1164820
22. AJ Weiss, E Weinstein, Fundamental limitations in passive time delay estimation-part I: narrow-band systems. IEEE Trans Acoust Speech Signal Process. **32**(5), 1064–1078 (1984). doi:10.1109/TASSP.1984.1164429
23. Y Chan, KC Ho, A simple and efficient estimator for hyperbolic location. IEEE Trans Signal Process. **42**(8), 1905–1915 (1994). doi:10.1109/78.301830
24. Y Huang, J Benesty, GW Elko, RM Mersereau, Real-time passive source localization: a practical linear-correction least squares approach. IEEE Trans Speech Audio Process. **9**(8), 943–956 (2001). doi:10.1109/89.966097
25. K Cheung, H Ho, A multidimensional scaling framework for mobile location using time-of-arrival measurements. IEEE Trans Signal Process. **53**(2), 460–470 (2005)
26. B Alavi, K Pahlavan, Modeling of the TOA-based distance measurement error using UWB indoor radio measurements. IEEE Commun Lett. **10**(4), 275–277 (2006). doi:10.1109/LCOMM.2006.1613745
27. J Riba, A Urruela, A robust multipath mitigation technique for time-of-arrival estimation, in *Proceedings of the IEEE Vehicular Technology Conference*, 1297–1301 (2002)
28. *IEEE, Std. 802.11a-2007 Part 11: Wireless LAN Medium Access Control (MAC) and Physical Layer (PHY) specifications*, IEEE Std http://www.ieee.org (2007)
29. TM Schmidl, DC Cox, Robust frequency and timing synchronization for OFDM. IEEE Trans Commun. **45**(12), 1613–1621 (1997). doi:10.1109/26.650240
30. J Medbo, P Schramm, Channel models for HIPERLAN/2, ETSI/BRAN, document no. 3ERI085B (1998)
31. I Guvenc, C-C Chong, F Watanabe, H Inamura, NLOS identification and weighted least-squares localization for UWB systems using multipath channel statistics. EURASIP J Adv Signal Process. **2008**, 1–14 (2008)
32. V Dizdarevic, K Witrisal, On impact of topology and cost function on LSE position determination in wireless networks, in *Proceedings of the Workshop on Positioning, Navigation, and Communication*, 129–138 (2006)
33. HL Van Trees, *Detection, Estimation, and Modulation Theory, Part I* (Wiley-Interscience, New York, 2001)

doi:10.1186/1687-1499-2011-189
Cite this article as: Yen and Voltz: **Indoor positioning based on statistical multipath channel modeling.** *EURASIP Journal on Wireless Communications and Networking* 2011 **2011**:189.